nature neuroscience

A discrete alcohol pocket involved in GIRK channel activation

Prafulla Aryal[1,2], Hay Dvir[3], Senyon Choe[2,3] & Paul A Slesinger[1,2]

Ethanol modifies neural activity in the brain by modulating ion channels. Ethanol activates G protein–gated inwardly rectifying K^+ channels, but the molecular mechanism is not well understood. Here, we used a crystal structure of a mouse inward rectifier containing a bound alcohol and structure-based mutagenesis to probe a putative alcohol-binding pocket located in the cytoplasmic domains of GIRK channels. Substitutions with bulkier side-chains in the alcohol-binding pocket reduced or eliminated activation by alcohols. By contrast, alcohols inhibited constitutively open channels, such as IRK1 or GIRK2 engineered to strongly bind PIP_2. Mutations in the hydrophobic alcohol-binding pocket of these channels had no effect on alcohol-dependent inhibition, suggesting an alternate site is involved in inhibition. Comparison of high-resolution structures of inwardly rectifying K^+ channels suggests a model for activation of GIRK channels using this hydrophobic alcohol-binding pocket. These results provide a tool for developing therapeutic compounds that could mitigate the effects of alcohol.

Many ligand-gated ion channels, such as those gated by GABA, NMDA, glycine, acetylcholine and serotonin, are responsive to ethanol and other alcohols[1–4]. Initially, alcohol was hypothesized to indirectly alter the function of channels by changing the fluidity of the lipid bilayer[5]. More recent studies, however, suggest that alcohol acts directly through a physical binding pocket located in the channel protein[1,6]. In addition to ligand-gated channels, alcohols also modulate potassium channels[7–9]. For example, ethanol activates G protein–gated inwardly rectifying potassium (GIRK or Kir3) channels[7,8]. Behavioral studies have shown that mice lacking GIRK2 channels have diminished ethanol-dependent analgesia[10] and consume more ethanol than wild-type mice[11], suggesting a functional role for GIRK channels in response to alcohols *in vivo*.

GIRK channels are also activated following stimulation of G protein–coupled receptors (GPCRs) such as m2 muscarinic receptors (m2Rs). The mechanism of G protein activation has been extensively studied. Agonist binding to the GPCR leads to activation of the pertussis toxin–sensitive G protein heterotrimer ($G\alpha\beta\gamma$), allowing the $G\beta\gamma$ subunits to associate directly with the channel and induce channel activation[12,13]. Mutagenesis and chimeric studies have identified several regions in the cytoplasmic domains of GIRK channels that are involved in $G\beta\gamma$ binding and activation[14–19]. Notably, pertussis toxin treatment, which prevents GPCR-mediated G protein activation of GIRK channels, does not prevent alcohol activation[8]. These experiments suggest that alcohol activation occurs through a mechanism that is distinct from G protein activation.

Similar to GABA-gated ion channels, a physical pocket in the channel with a defined cutoff is postulated to mediate alcohol activation of GIRK channels. Alcohols with a carbon chain length of up to four carbons (that is, methanol, ethanol, 1-propanol and 1-butanol) activate GIRK1/2 heteromeric channels, whereas longer alcohols inhibit the channels[7,8]. This cutoff effect suggests that there are physical constraints, possibly linked to the length or hydrophobicity of the alcohol, that determine the sensitivity to alcohol modulation[1,8]. However, the molecular mechanism underlying alcohol activation of GIRK channels is not known. Mutagenesis studies of GIRK2 channels have implicated the distal C-terminal cytoplasmic domain in activation by alcohol[7,20], but these studies did not reveal a physical alcohol-binding pocket in the channel.

Recently, we described a high-resolution structure of the cytoplasmic domains of a G protein–insensitive inwardly rectifying potassium channel (IRK1 or Kir2.1) that contained bound alcohols[21]. The alcohol, 2-methyl-2,4-pentanediol (MPD), is bound to four similar solvent-accessible hydrophobic pockets, each formed by two adjacent subunits of the tetramer. This IRK1-bound pocket has features that are similar to the structure of an odorant alcohol-binding protein, LUSH, that was crystallized with ethanol[22]. In both structures, the alcohol pocket is formed by hydrophobic amino acids and hydrogen-bonding polar groups. Thus, the hydrophobic alcohol-bound pocket in IRK1 is a putative site for modulation by alcohols. Because the crystal structure of the cytoplasmic domain of GIRK1 or GIRK2 channels is very similar to that of IRK1 (refs. 23–25), we hypothesize that GIRK channels also possess cytoplasmic hydrophobic alcohol-binding pockets that are involved in alcohol-dependent activation.

RESULTS

Conservation of MPD-bound pocket in IRK1 and GIRK2

Recently, we found that a high-resolution structure of the IRK1 cytoplasmic domains contains bound alcohols (which we refer to

[1]Peptide Biology Laboratory, The Salk Institute for Biological Studies, La Jolla, California, USA. [2]Graduate Program in Biology, Division of Biology, University of California, San Diego, La Jolla, California, USA. [3]Structural Biology Laboratory, The Salk Institute for Biological Studies, La Jolla, California, USA. Correspondence should be addressed to P.A.S. (slesinger@salk.edu) or S.C. (choe@salk.edu).

Received 7 April; accepted 3 June; published online 28 June 2009; doi:10.1038/nn.2358

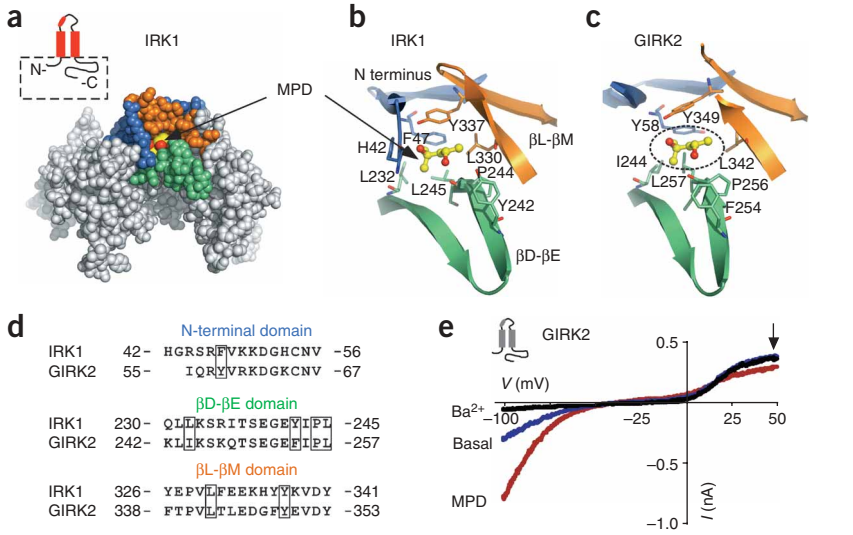

Figure 1 A conserved alcohol-binding pocket in IRK1 and GIRK2 channels. (**a**) Space-filling model of the cytoplasmic domains from two subunits of IRK1 in complex with an alcohol, MPD. The pocket for MPD consists of three structural elements: the N-terminal domain (blue), the βL-βM ribbon (orange) from one subunit and the βD-βE ribbon (green) from an adjacent subunit. Inset, schematic of IRK1 (red) showing the major structural elements of the subunit, including the pore loop and helix, two transmembrane domains, and the N- and C-terminals used in the structure (dashed box). (**b**,**c**) Detailed structural views of amino acids forming the hydrophobic alcohol pocket of IRK1 with MPD (**b**) and a putative hydrophobic alcohol pocket in GIRK2 (**c**). Amino acid residues shown in stick format are colored according to the domain they originate from; MPD is shown in ball-and-stick format. The putative position of MPD in GIRK2 (dashed circle) was obtained by superposition of two adjacent cytoplasmic domains from IRK1 structure and corresponding subunits from GIRK2 structure. (**d**) Sequence alignment for the three domains comprising the hydrophobic alcohol pocket in IRK1 and GIRK2 channels. Boxes indicate amino acids that form hydrophobic and hydrogen-bond interactions in IRK1-MPD and are conserved in GIRK2. HG in the N-terminal domain of IRK1 indicates the polypeptide linker in the IRK1-MPD structure. (**e**) Current-voltage plots for GIRK2 channels recorded in the presence of 20K solution (blue), (see Online Methods), 20K and 1 mM Ba^{2+} (black) or 20K and 100 mM MPD (red). Currents were elicited by voltage ramps from −100 mV to +50 mV. MPD-induced current was 246% ± 27% ($n = 5$, mean and s.e.m.) of basal K^+ current (Ba^{2+} sensitive).

here as IRK1-MPD)[21]. The alcohol-binding pocket in the IRK1-MPD complex is formed by hydrophobic amino acid side chains from three different domains: the N terminus, the βD-βE ribbon and the βL-βM ribbon (**Fig. 1a**,**b**)[21]. There are seven amino acids that interact with MPD[21]. Of these, the hydrophobic side chains of F47, L232, L245 and L330, and Y337 point toward the pocket. In addition to the hydrophobic environment of the pocket, hydrogen bonds may form between one of the hydroxyl groups of MPD and a hydrogen bonding triangle between the backbone carbonyl of P244 and the hydroxyl group of Y242 via a water and between the second hydroxyl group of MPD and the hydroxyl group of Y337 (ref. 21).

We compared the high-resolution structure of IRK1 with that of GIRK2 (ref. 25) and identified the putative alcohol-binding pocket in GIRK2. The hydrophobic pocket in GIRK2 has substantial conservation with the amino acids that line the pocket in IRK1. The hydrophobic pocket in GIRK2 is large enough to accommodate MPD, similar to IRK1 (**Fig. 1c**,**d**).

MPD activates GIRK2 channels similar to primary alcohols

To test whether the hydrophobic pocket in GIRK2 is the site for alcohol-mediated activation, we first investigated whether GIRK2 channels are sensitive to MPD modulation. Although primary alcohols up to the size of butanol (1-butanol, four carbons) activate GIRK1/2 channels[7,8], the effect of MPD with five backbone carbons is unknown. GIRK2 channels expressed in HEK-293T cells produced a small inwardly rectifying basal K^+ current that was inhibited by extracellular Ba^{2+} (**Fig. 1e**). Bath application of MPD (100 mM) increased the amplitude of the inwardly rectifying current (**Fig. 1e**), indicating that MPD activates GIRK channels. In addition, MPD appeared to inhibit an endogenous voltage-gated outward current at positive potentials (**Fig. 1e**), which is probably a voltage-gated K^+ channel[9]. All three alcohols activated GIRK2 channels at 10 mM and showed a steep increase in activation around 100 mM (**Fig. 2a**). The activation curve for MPD fell between that of ethanol and 1-propanol (**Fig. 2b**) and did not reach a maximum, similar to the findings of previous studies[7,8].

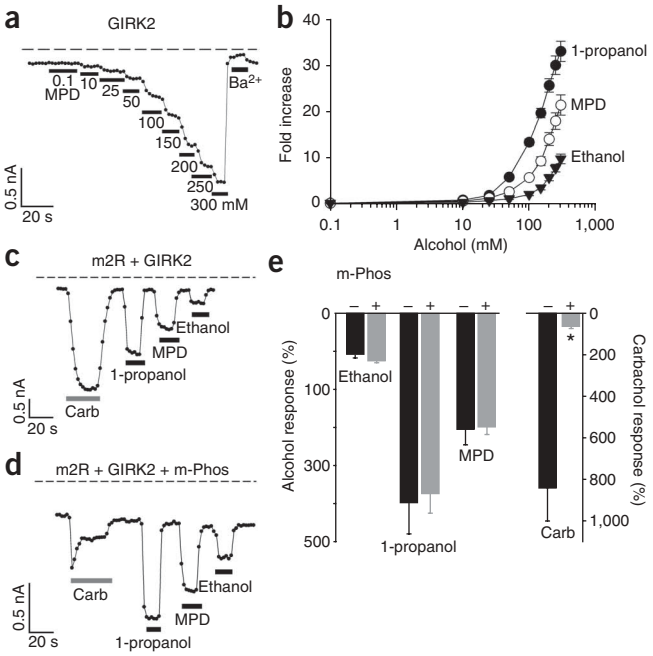

Figure 2 MPD activates GIRK2 in a manner similar to other alcohols. (**a**) The inward current through GIRK2 channels plotted as a function of time (at −100 mV) shows the response to the increasing concentrations of MPD and to 1 mM Ba^{2+}. Dashed line shows zero current level. (**b**) Dose-response curves are shown for MPD ($n = 6$), 1-propanol ($n = 6$) and ethanol ($n = 6$). The fold-increase was calculated by normalizing to the basal K^+ current (Ba^{2+} sensitive). (**c**,**d**) Chelating Gβγ with m-Phos attenuated m2R-mediated, but not alcohol-mediated, activation of GIRK2. Current responses recorded at −100 mV are shown for m2R and GIRK2 (**c**) or m2R, GIRK2 and m-Phos (**d**) in response to 100 mM 1-propanol, 100 mM MPD, 100 mM ethanol or 5 μM carbachol (Carb). (**e**) Bar graphs show the mean percentage alcohol and carbachol responses (± s.e.m.), normalized to the Ba^{2+}-sensitive basal current, in the absence (solid, $n = 4$) or presence of m-Phos (gray, $n = 7$). Asterisk indicates statistical significant difference from wild type ($P < 0.05$).

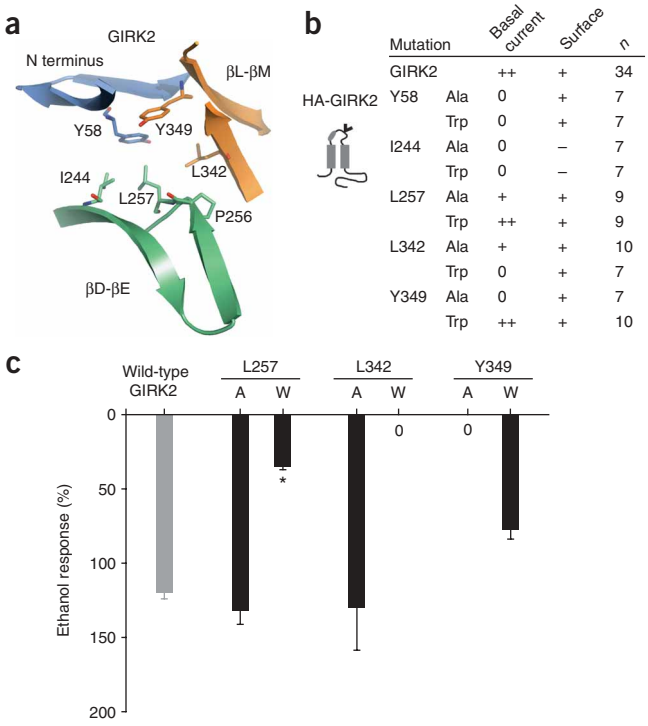

Mutation		Basal current	Surface	n
GIRK2		++	+	34
Y58	Ala	0	+	7
	Trp	0	+	7
I244	Ala	0	–	7
	Trp	0	–	7
L257	Ala	+	+	9
	Trp	++	+	9
L342	Ala	+	+	10
	Trp	0	+	7
Y349	Ala	0	+	7
	Trp	++	+	10

Figure 3 Alanine/tryptophan scan of the hydrophobic alcohol-binding pocket in GIRK2. (**a**) Ribbon structure shows amino acids that line the hydrophobic alcohol pocket in GIRK2. (**b**) Summary table of alanine (Ala)/tryptophan (Trp) mutagenesis. Basal K^+ currents (Ba^{2+} sensitive) were divided into three groups: <-1 pA pF^{-1} (0), -1 to -5 pA pF^{-1} (+) and >-5 pA pF^{-1} (++) (n = number of recordings). Surface expression on the plasma membrane was assessed in separate experiments with HA-tagged channels; detected on the surface (+) or detected only in cytoplasm (–) (see **Supplementary Fig. 2**). Schematic shows the location of the HA tag in GIRK2 (gray). (**c**) Bar graph shows the mean ethanol percentage response, normalized to the basal K^+ current, for different mutant channels (± s.e.m.). L257W showed a significant statistical decrease in ethanol response ($^*P < 0.05$ versus wild type).

These results indicate that MPD activates GIRK2 in a similar manner to other small n-alcohols. Notably, 1-pentanol, which has five backbone carbons, similar to MPD, predominantly inhibited GIRK2 channels (**Supplementary Fig. 1**). Therefore, a large diol, such as MPD, activates GIRK2 channels in a similar manner to small primary alcohols, such as ethanol, but is different from 1-pentanol (see Discussion).

Pertussis toxin treatment does not prevent ethanol activation of GIRK channels, indicating that GPCR coupling to G proteins is not involved[8]. To rule out the possibility that alcohols activate GIRK channels by directly stimulating G protein heterotrimers and liberating Gβγ subunits, we measured the alcohol response of GIRK2 channels in cells coexpressing a myristoylated form of phosducin (m-Phos) that chelates Gβγ following stimulation of GPCRs[26]. Compared with controls, carbachol application led to smaller and rapidly desensitizing m2R-evoked GIRK2 currents in cells coexpressing m-Phos (**Fig. 2c–e**). All three alcohols, on the other hand, activated GIRK2 channels to the same extent in the presence of m-Phos (**Fig. 2d,e**). Thus, alcohol-dependent activation of GIRK2 channels does not appear to require free Gβγ subunits. Together, these results support the interpretation that alcohols directly activate GIRK channels through a physical alcohol-bound pocket.

Role for hydrophobic pocket in alcohol activation

To determine whether the hydrophobic pocket in GIRK2 mediates alcohol activation, we examined the effects of the side-chain volume by substituting an amino acid with a small (alanine) or large (tryptophan) side chain (**Fig. 3a,b**). Six mutants did not express basal K^+ currents (<-1 pA pF^{-1}; **Fig. 3b**). In mutant channels engineered with an extracellular hemagglutinin (HA) tag, we investigated whether the lack of basal current was the result of a trafficking defect using confocal microscopy. Four mutant channels, HA-GIRK2-Y58W, HA-GIRK2-Y58A, HA-GIRK2-L342W and HA-GIRK2-Y349A, were expressed on the plasma membrane, but did not conduct currents (**Fig. 3b** and **Supplementary Fig. 2**). Mutations at GIRK2-I244 impaired expression on the membrane surface (**Fig. 3b**). These findings suggest the hydrophobic pocket in GIRK2 is important for channel gating and/or assembly in the absence of alcohol. Four other mutants, GIRK2-L257A, GIRK2-L257W, GIRK2-L342A and GIRK2-Y349W, produced functional channels that were activated by ethanol (**Fig. 3c**). However, GIRK2-L257W showed significantly smaller ethanol-activated currents ($P < 0.05$ versus wild type; **Fig. 3c**), suggesting that the leucine at position 257 in the βD-βE ribbon is an important residue that is required for alcohol-dependent activation of GIRK2 channels.

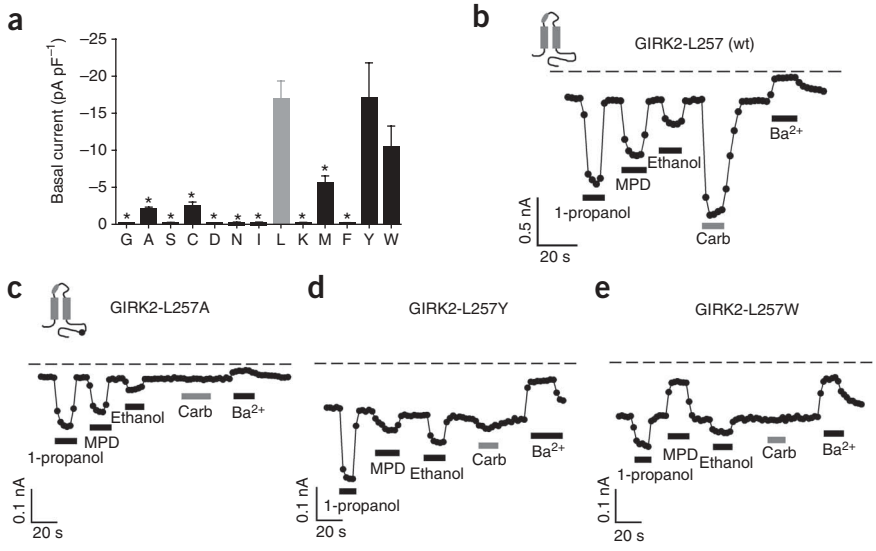

Figure 4 Comprehensive mutagenesis of GIRK2-L257 in the βD-βE ribbon of hydrophobic alcohol-binding pocket reveals changes in alcohol- and Gβγ-activated currents. (**a**) Bar graph shows the mean (± s.e.m.) amplitude of basal K^+ current (Ba^{2+} sensitive) for substitutions of increasing molecular side-chain volume at GIRK2-L257: glycine ($n = 7$, G), alanine ($n = 9$, A), serine ($n = 7$, S), cysteine ($n = 8$, C), aspartic acid ($n = 7$, D), asparagine ($n = 6$, N), isoleucine ($n = 7$, I), leucine (wt; $n = 34$, L, gray bar), lysine ($n = 7$, K), methionine ($n = 8$, M), phenylalanine ($n = 7$, F), tyrosine ($n = 9$, Y) and tryptophan ($n = 9$, W). Asterisks indicate statistical difference ($P < 0.05$ versus leucine). (**b–e**) Inward K^+ currents for wild-type GIRK2 (**b**) and the indicated GIRK2-L257 mutants (**c–e**) in response to 100 mM 1-propanol, 100 mM MPD, 100 mM ethanol, 5 μM carbachol or 1 mM Ba^{2+}. Inset shows the approximate position of the C-terminal mutation.

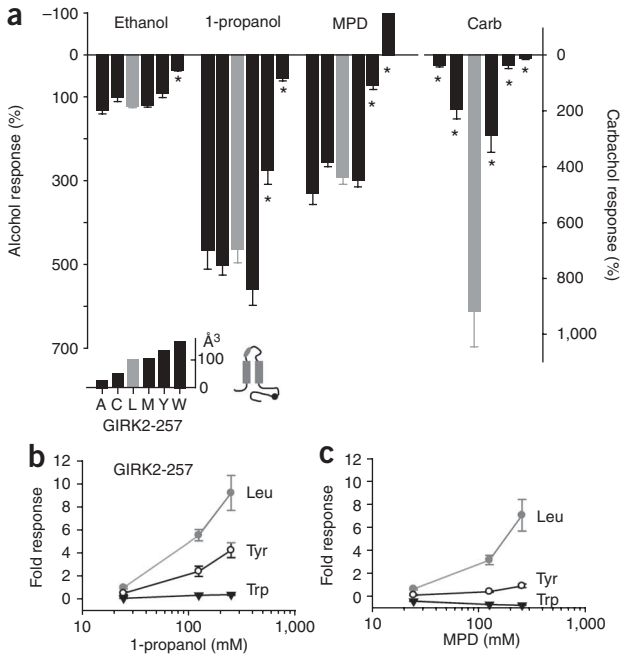

Figure 5 Reduced alcohol activation with increasing bulkiness of amino acid substitutions at GIRK2-L257. (**a**) Bar graph shows the mean percentage response to different alcohols and carbachol (± s.e.m.), normalized to the basal K^+ current (Ba^{2+} sensitive). Upward response indicates inhibition. Amino acid substitutions are arranged by increasing side-chain volume (Å^3, see inset). Asterisks indicate significant statistical difference ($P < 0.05$ versus leucine). (**b**,**c**) Dose-response curves are shown for GIRK2-L257, GIRK2-L257Y and GIRK2-L257W channels for 1-propanol (**b**) and MPD (**c**). Note the suppression of alcohol activation over a range of concentrations. Leu, leucine; Trp, tryptophan; Tyr, tyrosine.

In the IRK1-MPD structure, L245, which is homologous to L257, is positioned at the base of the pocket and interacts intimately with MPD. The decrease in ethanol-activated current of GIRK2-L257W raised the possibility that amino acids with bulky side chains might generally interfere with alcohol activation. We systematically evaluated the effect of substituting 12 different amino acids of increasing molecular side-chain volume in GIRK2-L257. Of the 12 mutant channels, 5 were expressed (>−1 pA pF^{-1}) and could be examined for possible changes in alcohol-mediated activation (**Fig. 4a**). The magnitude and rank order (1-propanol > MPD > ethanol) for alcohol activation with smaller molecular volume substitutions, such as alanine, cysteine and methionine, were indistinguishable from wild-type leucine in GIRK2 channels (**Fig. 4b**,**c**). On the other hand, GIRK2-L257Y reduced 1-propanol and MPD, but not ethanol, activation, whereas GIRK2-L257W affected ethanol-, 1-propanol– and MPD-dependent activation (**Figs. 4d**,**e** and **5a**). Notably, 100 mM MPD no longer activated and instead inhibited the basal currents for GIRK2-L257W (**Figs. 4e** and **5a**). For GIRK2-L257Y and GIRK2-L257W, the decrease in alcohol activation was observed at a full range of concentrations (25, 125 and 250 mM) for 1-propanol or MPD (**Fig. 5b**,**c**), indicating a substantial impairment in alcohol sensitivity. In addition to the change in alcohol response, mutations at L257 also reduced the m2R-mediated currents (**Figs. 4c–e** and **5a**), indicating that L257 is involved in both alcohol-mediated and Gβγ-mediated activation (see Discussion). Taken together, these results demonstrate that increasing the side-chain volume at L257 leads to a progressive loss in alcohol-mediated activation (**Fig. 5a**). A switch in alcohol activation occurred with an increase in volume from leucine (101 Å^3) in the wild type to tyrosine (133 Å^3) or tryptophan (168 Å^3). In addition, bulky substitutions at L257 affected larger alcohols (MPD) more than smaller alcohols (ethanol), suggesting the molecular volume of the pocket is an important determinant of alcohol specificity.

Because alcohol activation is a property of most types of GIRK channels[7,8], we reasoned that a homologous mutation in a related GIRK channel would also alter the response to alcohols. To test this idea, we investigated the effects of mutating L252 in GIRK4*. GIRK4* contains a mutation in the pore helix (S143T) that enhances channel activity without affecting surface expression[27]. Substituting alanine (26 Å^3), tyrosine (133 Å^3) or tryptophan (168 Å^3) at L252 in GIRK4* channels did not change the basal K^+ currents (**Fig. 6a**). Similar to mutations of L257 in GIRK2, tryptophan and tyrosine substitutions in GIRK4* decreased ethanol, 1-propanol and MPD activation, as compared with L252A, with 1-propanol now inhibiting GIRK4*-L252W (**Fig. 6b–f**). In contrast with GIRK2, however, MPD activation of GIRK4*-L252W was not significantly different from wild type ($P > 0.05$; **Fig. 6e**,**f**). Mutating GIRK4*-L252 also significantly reduced m2R-activated GIRK currents ($P < 0.05$; **Fig. 6c–f**). Thus, the putative

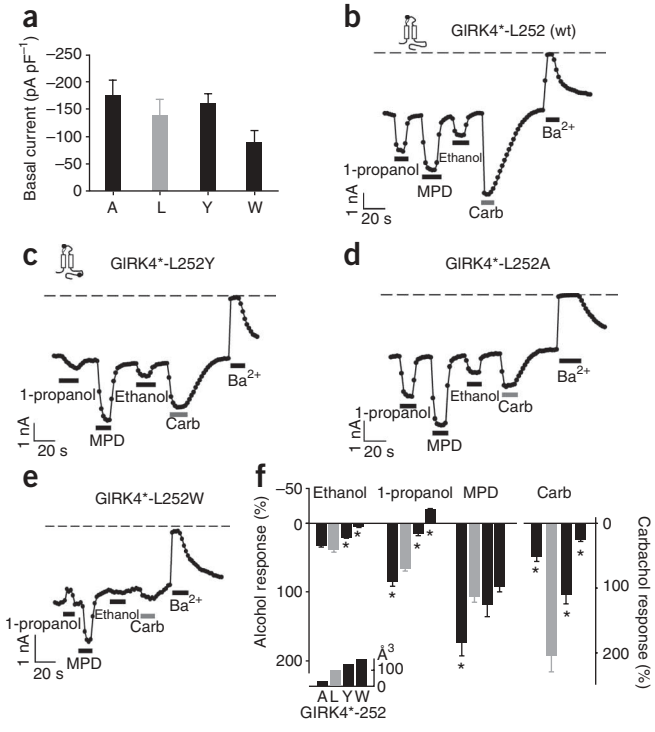

Figure 6 Mutations in the hydrophobic alcohol-binding pocket of GIRK4* alter alcohol-activated currents. (**a**) Mean basal K^+ currents (Ba^{2+} sensitive) measured for alanine ($n = 8$), leucine (wt; gray bar, $n = 8$), tyrosine ($n = 8$) and tryptophan ($n = 8$) substitutions at GIRK4*-L252. There were no statistical differences in basal currents ($P > 0.05$ versus Leu). (**b**–**e**) Inward K^+ currents for GIRK4* (**b**) and different GIRK4*-L252 mutants (**c**–**e**) in response to 100 mM 1-propanol, 100 mM MPD, 100 mM ethanol, 5 μM carbachol or 1 mM Ba^{2+}. (**f**) Bar graphs show the mean percentage responses to different alcohols and carbachol, normalized to the basal K^+ current (Ba^{2+} sensitive). Amino acid substitutions are arranged by increasing side-chain volume (Å^3) (see inset). Asterisks indicate significant difference ($P < 0.05$ versus Leu). Channel schematics show the approximate position of the pore-helix (white ellipse) mutation for making GIRK4* and the C-terminal mutation (black circle). All values are mean ± s.e.m.

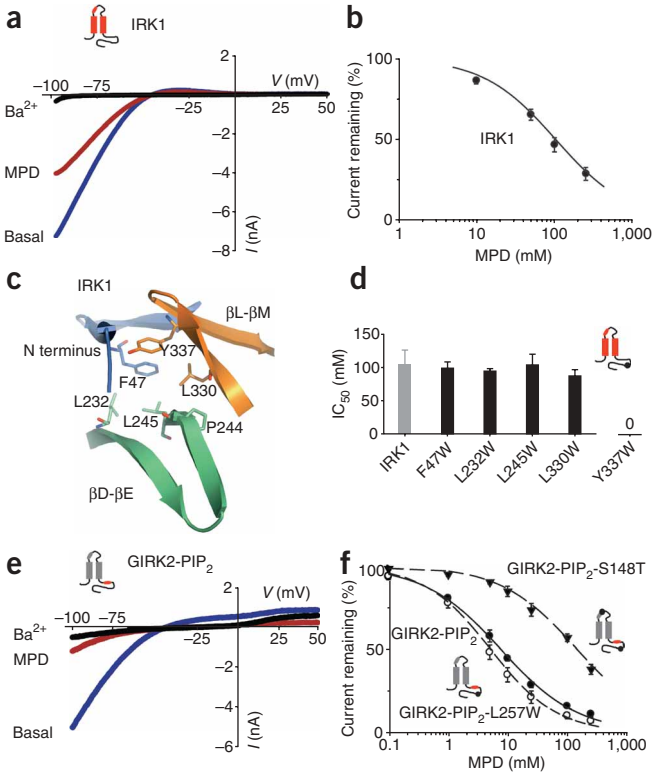

Figure 7 Mutations in the hydrophobic alcohol-binding pocket of IRK1 have no effect on alcohol-dependent inhibition. (**a**) Current-voltage plots for IRK1 channels are shown for 20K (blue), 20K and 1 mM Ba^{2+} (black) or 20K and 100 mM MPD (red). MPD inhibited the basal K^+ current (Ba^{2+} sensitive) by 53.1% ± 4.1% ($n = 8$). (**b**) Dose-response curve for MPD inhibition of IRK1 channel. The smooth curve shows the best fit using the Hill equation, with an IC_{50} of 104 ± 23 mM and Hill coefficient of 0.93 ± 0.03 ($n = 8$). (**c**) Structural view of amino acids that line the hydrophobic alcohol pocket in IRK1. (**d**) Bar graph shows mean IC_{50}s for MPD-dependent inhibition of IRK1 ($n = 8$), IRK1-F47W ($n = 7$), IRK1-L232W ($n = 7$), IRK1-L245W ($n = 6$) and IRK1-L330W ($n = 6$). There was no statistically significant difference compared with wild-type IRK1 ($P > 0.05$). (**e**) Current-voltage plots are shown for GIRK2-PIP_2 (GIRK2 engineered with high-affinity PIP_2 binding domain from IRK1) channels recorded in the presence of 20K (blue), 20K and 1 mM Ba^{2+} (black) or 20K and 100 mM MPD (red). (**f**) Dose-response curves for MPD-dependent inhibition of GIRK2-PIP_2 (solid circle), GIRK2-PIP_2-L257W (open circle) and GIRK2-PIP_2-S148T (solid triangle). The smooth curves show the best fit using the Hill equation and have IC_{50}s and Hill coefficients of 7.7 ± 1.0 mM and 0.66 ± 0.03 ($n = 5$) for GIRK2-PIP_2, 5.2 ± 1.0 mM and 0.77 ± 0.04 ($n = 5$) for GIRK2-PIP_2-L257W, and 147.0 ± 31.5 mM and 0.67 ± 0.05 ($n = 6$) for GIRK2-PIP_2–S148T. All values are mean ± s.e.m.

hydrophobic alcohol-binding pocket in GIRK4* is important for mediating alcohol activation, but GIRK4* may accommodate MPD differently than GIRK2 (see Discussion).

Mutations of MPD pocket do not alter alcohol inhibition

MPD is bound to a hydrophobic pocket in the crystal structure of IRK1, suggesting that MPD might inhibit IRK1 channels, similar to other alcohols[7,8]. Bath applying 100 mM MPD inhibited nearly 50% the basal inwardly rectifying K^+ current through IRK1 channels (**Fig. 7a**). The MPD inhibition was dose dependent and had an IC_{50} (the concentration required to inhibit 50% of the current) of 104 ± 23 mM and a Hill coefficient of 0.93 ± 0.02 ($n = 8$; **Fig. 7b**). We next investigated whether tryptophan substitutions in the hydrophobic alcohol-binding pocket of IRK1 altered alcohol-dependent inhibition (**Fig. 7c**). IRK1-F47W, IRK1-L232W, IRK1-L245W and IRK1-L330W, but not IRK1-Y337W, produced a substantial basal K^+ current (data not shown). Similar to wild-type IRK1, MPD inhibited the basal currents of mutant channels in a dose-dependent manner. The IC_{50} for MPD inhibition was indistinguishable among the different IRK1 mutants (**Fig. 7d**). Furthermore, IRK1-L245W mutation did not alter inhibition by ethanol, 1-propanol or 1-butanol (data not shown). Thus, mutations at the hydrophobic pocket of IRK1 channels do not appear to alter the sensitivity to inhibition by alcohols.

IRK1 channels are constitutively open, producing a large basal K^+ current. We speculated that alcohols might therefore inhibit GIRK channels that are engineered to be constitutively open. We introduced a high-affinity PIP_2 site that has previously been shown to produce a large basal current[28,29] (GIRK2-PIP_2). In contrast with wild-type GIRK2, GIRK2-PIP_2 showed large basal currents, as expected (–530 ± 197 pA pF^{-1}, $n = 5$). Application of 100 mM MPD inhibited the basal K^+ current of GIRK2-PIP_2 (**Fig. 7e**). Similar to IRK1, we hypothesized that mutating L257 to tryptophan in GIRK2-PIP_2 would have no effect in alcohol-mediated inhibition. Accordingly, GIRK2-PIP_2-L257W produced large basal K^+ currents (–363 ± 182 pA pF^{-1}, $n = 6$) that were inhibited by MPD, similar to GIRK2-PIP_2 channels (**Fig. 7f**). We conclude that the hydrophobic alcohol-binding pocket in IRK1 or GIRK2 is not involved in alcohol-dependent inhibition. Furthermore, these results indicate that constitutively open inwardly rectifying K^+ channels are not activated further by alcohols.

While investigating alcohol modulation of GIRK4*, we found that 1-butanol activated GIRK4*, in contrast with its inhibition of wild-type GIRK4 (**Supplementary Fig. 3**) or GIRK1/4 heterotetramers[7,8]. GIRK4 and GIRK4* differ by a point mutation (S143T) in the pore helix[27], suggesting that S143T may regulate sensitivity to alcohol inhibition. To assess whether this site is generally involved in alcohol-mediated inhibition of GIRK channels, we introduced a threonine at the equivalent serine (S148T) in GIRK2-PIP_2 channels. As predicted, GIRK2-PIP_2-S148T significantly shifted the IC_{50} for MPD-dependent inhibition compared with GIRK2-PIP_2 ($P < 0.05$; **Fig. 7f**). Taken together, these experiments implicate amino acids in the pore helix in regulating the extent of alcohol-dependent inhibition and support the conclusion that the cytoplasmic alcohol-binding pocket mediates alcohol-dependent activation, but not inhibition, of GIRK channels.

DISCUSSION

On the basis of high-resolution channel structures and functional mutagenesis, we have identified a physical site for alcohol-mediated activation of GIRK channels. Amino acid substitutions that increased the molecular side-chain volume at a conserved leucine in the βD-βE ribbon of the hydrophobic pocket of GIRK2 decreased alcohol-mediated activation of GIRK channels (**Fig. 8a**). In particular, two substitutions, tryptophan and tyrosine, at the leucine in the hydrophobic pocket of GIRK2 (L257) and GIRK4* (L252) channels produced a progressive loss in alcohol activation. For GIRK4*, alanine substitution increased the amplitude of alcohol-activated currents. Thus, increasing or decreasing the volume of the pocket by altering the amino acid side-chain produced changes in alcohol activation. Similarly, the size of the putative alcohol-binding pocket in $GABA_A$ α1 and glycine receptors is important for determining modulation by alcohol and other small anesthetics. Increasing the bulkiness of amino acids in the putative alcohol-binding pocket of these channels eliminates modulation by ethanol[1] or isofluorane[30]. In contrast, decreasing the size of amino acids in the same region of the decanol-insensitive

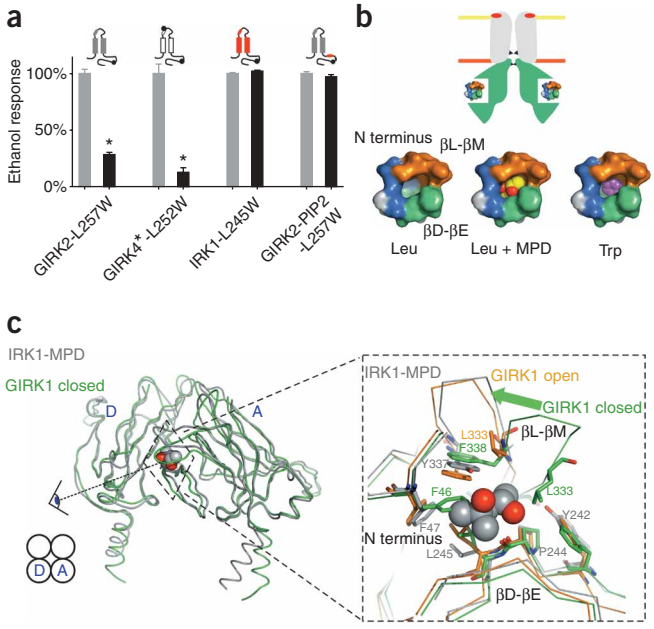

Figure 8 Model for alcohol-dependent activation of GIRK channels. (**a**) Bar graph shows the mean percentage ethanol response (activation or inhibition normalized to wild type) for a tryptophan mutation in four different channels: GIRK2-L257W ($n = 9$), GIRK4-L252W ($n = 8$), IRK1-L245W ($n = 8$) and GIRK2-PIP_2-L257W ($n = 5$). Mutation in the alcohol-binding pocket affected activation (* $P < 0.05$ versus wild type), but not inhibition, of GIRK channels. (**b**) Top, schematic of inward rectifier shows the location of the alcohol-binding pocket in the cytoplasmic domains, two gates (G loop and M2 transmembrane, black triangles) and pore-helix region (red ellipse). PIP_2 is enriched in the lower leaflet of bilayer (orange). Bottom, molecular surface representations of the alcohol pocket without (Leu), with MPD (Leu + MPD) and modeled with L257W (Trp), using the IRK1-MPD structure as a guide. (**c**) Left, alignment of the putative closed state of GIRK1 chimeric channel (GIRK1 closed, green) with the IRK1-MPD structure (gray). Spaghetti structures show two adjacent cytoplasmic subunits (subunits D and A) and the hydrophobic alcohol pocket at the cytoplasmic subunit interface. Right, zoom shows alignment of the N-terminal domain, βD-βE and βL-βM ribbons from the IRK1-MPD (gray), GIRK1 open (orange) and GIRK1 closed (green) structures. IRK1-MPD aligns better with the putative open state of GIRK1. Note the substantial displacement in the βL-βM ribbon (arrow) and the side chains of hydrophobic amino acids in the two structures. GIRK1 closed, but not GIRK1 open, has a collapsed alcohol-binding pocket, as a result of the interaction and rotation of F46 (IRK1-F47), L246 (IRK1-L245) and F338 (IRK1-Y337). GIRK1-L333 in the βL-βM domain, implicated previously in Gβγ gating of GIRK channels[17–19], is shown for reference.

GABA ρ1 receptors enables potentiation by decanol[1,6]. Together with our findings, these studies suggest that physical pockets of defined dimensions can be probed with mutations that change the dimension of the alcohol-binding sites. Using the IRK1-MPD structure as a guide, we estimated the volume of the hydrophobic alcohol-binding pocket of GIRK channels to be ~250 Å^3, which is large enough to accommodate bulky alcohols such as MPD (~130 Å^3; **Fig. 8b**). A tryptophan mutation in the pocket would decrease the volume that could potentially occlude larger alcohols (**Fig. 8b**). In addition, the sensitivity to activation may be different between GIRK2 and GIRK4* channels. For example, tryptophan substitution in GIRK2 eliminated MPD activation, revealing inhibition of current. In GIRK4*, tryptophan substitution eliminated 1-propanol activation, but showed only a substantial decrease in MPD activation when comparing alanine with tryptophan substitutions. One possible explanation is that MPD fits differently in the alcohol pocket of GIRK4*, which could be revealed in a GIRK4 structure in complex with MPD.

The observations that mutations at the hydrophobic pocket did not alter alcohol-dependent inhibition of IRK1 and that S148T mutation (but not L257W) in GIRK2-PIP_2 decreased alcohol-dependent inhibition suggest that GIRK channels possess two different sites for alcohol modulation. In the Kirbac1.3 structure, the serine is located in the pore helix of Kirbac1.3 where there is no space for alcohol (**Supplementary Fig. 4**), suggesting that S148 regulates sensitivity to inhibition, but does not form the binding site. Alcohols might interfere with ion permeation or possibly with gating at the transmembrane domains, similar to voltage-gated K channels[9]. Another possibility is that alcohols inhibit the channel by altering the fluidity of the lipid membrane[5] and/or decreasing interactions with PIP_2, which is required for channel function[31].

Notably, although 1-octanol inhibits GIRK channels, coapplication of 1-octanol with ethanol has no effect on ethanol-mediated activation, also raising the possibility of a second site for inhibition[7]. The net effect of alcohol modulation in GIRK channels would therefore be determined by the relative potencies of activation and inhibition. In support of this, we found that bath application of 1-pentanol inhibited GIRK2 channels, but induced a large current immediately after washout (**Supplementary Fig. 1**), revealing two components of alcohol modulation. It is notable that MPD predominantly activates GIRK channels, in contrast with large primary alcohols of similar size. A functional difference between diols and primary alcohols has been reported previously for NMDA channels[32]. The addition of a hydroxyl group may lead to decreased sensitivity to inhibition for GIRK channels. The presence of two sites for alcohol modulation also suggests that ascribing a cutoff number for alcohol activation of GIRK channels would not be accurate, in contrast with the determination of the cutoff number for $GABA_A$ channels[1,6,33].

Two different types of alcohol-bound protein structures have been solved previously, the enzymatic/catalytic alcohol dehydrogenase and the noncatalytic *Drosophila* odorant-binding protein LUSH. In alcohol dehydrogenase, primary alcohol is coordinated with Zn^{2+} in a hydrophobic pocket, where it catalyzes the oxidation of alcohol to aldehyde[34,35]. Mutagenesis studies in the pocket indicated that the bulkiness of the side chains in the hydrophobic pocket determines the alcohol specificity[36]. The high-resolution structure of LUSH in complex with small alcohols showed that, in addition to hydrophobic interactions, a network of hydrogen bonds help to stabilize alcohol in the alcohol-binding pocket[22,37]. The hydrophobic pocket in IRK1-MPD has many of the same features of these alcohol-binding pockets. First, hydrophobic amino acids form the pocket and interact intimately with hydrocarbons of the alcohol (**Fig. 1b**). In GIRK2, mutations of L257 to bulkier amino acids substantially reduced or eliminated alcohol-mediated activation. This finding is consistent with a role for hydrophobic side chains in determining the size of the alcohol-binding pocket. Second, the IRK1-MPD structure indicates that hydrogen-bonds form between MPD and the backbone carbonyl of P244, Y242 via a water and a hydroxyl of Y337 (**Fig. 1**)[21]. At the homologous position for IRK1-Y242, GIRK2 contains a phenylalanine (F254), which indicates that this hydrogen-bond triangle may not be essential. In addition, we found that MPD-mediated activation was not affected by a Y349W mutation at the homologous position of IRK1-Y337 (**Supplementary Fig. 5**). Therefore, it is possible that the carbonyl group of proline in the βD-βE ribbon is the linchpin that stabilizes alcohol in the pocket via hydrogen bonding. Unnatural amino acid mutagenesis[38] would be needed to further establish the importance of this hydrogen-bond interaction in stabilizing alcohol.

Although specific alcohol-induced conformational changes in the channel protein remain unknown, our structural analysis between the IRK1-MPD structure and that of the chimeric KirBac1.3-GIRK1 provides some new clues into channel gating[21,39]. Two different conformational states of GIRK have been described: a putative open state, resulting from the open position of the G loops in the cytoplasmic gate[24,39] (GIRK1 open; **Fig. 8c**), and a putative closed state (GIRK1 closed; **Fig. 8c**). We aligned the IRK1-MPD structure with these two different Kirbac1.3-GIRK1 structures and discovered that IRK1-MPD structure aligns better with the GIRK1 open in the hydrophobic alcohol-binding pocket (**Fig. 8c**). In contrast, the alignment with the GIRK1 closed structure showed marked differences in the hydrophobic alcohol pocket. In particular, the side chains from F46 in the N-terminal domain, L246 in the βD-βE ribbon and L333 in the βL-βM ribbon, fill the hydrophobic pocket of the putative closed state of GIRK1. In the open state, structural rearrangements of F46, L246, L333 and F338 occur, which would enable MPD to fit in the pocket.

On the basis of our mutagenesis data and structural analyses, we propose a tenable model for alcohol activation of GIRK channels. At rest, GIRK2 channels undergo infrequent structural rearrangements in the pocket that correlate with the open and closed positions of the channel's cytoplasmic gates, the G loops[24,39] and M2 transmembrane domains[40–42] (**Fig. 8b**,**c**). Alcohol entering the pocket could then stabilize the open conformation, leading to alcohol-activated currents. Bulky substitutions at L257/L252 of GIRK channels, located at the base of the alcohol pocket, would hinder alcohols from filling the pocket. Previous studies have shown that gating of GIRK channels requires PIP_2[28,31]. Similarly, alcohol-dependent activation may increase PIP_2 affinity for the channel, stabilizing an open confirmation. Thus, a PIP_2-activated GIRK channel would not be activated further by alcohol, as was observed with GIRK2-PIP_2 (**Fig. 7**). Future studies will need to investigate the molecular relationships between movement of the N-terminal domain, the βD-βE and βL-βM ribbons in the hydrophobic pocket, PIP_2 interactions, and the channel gates.

The alcohol-binding pocket may also be involved in Gβγ-dependent activation. Mutation of a conserved leucine (GIRK2-L344, GIRK4*L339, GIRK1-L333; **Fig. 8c**) to glutamic acid in the βL-βM ribbon of GIRK channels attenuates Gβγ activation[17–19]. We found that mutations in the βD-βE (L257) ribbon that altered alcohol-dependent activation also reduced Gβγ-dependent activation (**Figs. 4** and **5**). Together, these results suggest that conformational changes in the βD-βE and βL-βM structural elements, along with the N-terminal domain[43,44], may be central to both alcohol- and Gβγ-dependent activation. Notably, hydrophobic amino acids in the G protein Gβ subunit have been implicated in GIRK channel activation[45], which perhaps interact directly with the alcohol-binding pocket in GIRK.

METHODS

Methods and any associated references are available in the online version of the paper at http://www.nature.com/natureneuroscience/.

Accession codes. We used protein structures from the Protein Database, accession codes 2GIX (IRK1-MPD), 2E4F (GIRK2) and 2QKS (Kirbac1.3-GIRK1).

Note: Supplementary information is available on the Nature Neuroscience website.

ACKNOWLEDGMENTS

We would like to thank Y. Kurachi for GIRK2 coordinates, M. Lazdunsky for GIRK2 cDNA, D. Clapham for GIRK4 cDNA, N. Dascal for m-Phos cDNA, S. Pegan for initial discussions on structure of IRK1-MPD and members of the Slesinger laboratory for helpful comments. This work was funded, in part, by a pre-doctoral National Research Service Award from the National Institute on Alcohol Abuse and Alcoholism (F31AA017042, P.A.), by the National Institute on General Medical Sciences (R01GM056653, S.C.), and by the H.N. & Frances C. Berger Foundation and the Salk Institute for Biological Studies (P.A.S.). The content is solely the responsibility of the authors and does not necessarily represent the official views of the National Institute on Alcohol Abuse and Alcoholism or the National Institute on General Medical Sciences.

AUTHOR CONTRIBUTIONS

P.A.S. and P.A. designed the experiments and analyzed the data. P.A. conducted the molecular cloning, electrophysiology and imaging experiments. H.D. and P.A. collaborated on structural analysis and figure production. H.D. conducted modeling experiments. P.A., H.D. and P.A.S co-wrote and revised the manuscript. P.A.S and S.C. supervised the project.

Published online at http://www.nature.com/natureneuroscience/.
Reprints and permissions information is available online at http://www.nature.com/reprintsandpermissions/.

1. Mihic, S.J. *et al.* Sites of alcohol and volatile anaesthetic action on $GABA_A$ and glycine receptors. *Nature* **389**, 385–389 (1997).
2. Lovinger, D.M., White, G. & Weight, F.F. Ethanol inhibits NMDA-activated ion current in hippocampal neurons. *Science* **243**, 1721–1724 (1989).
3. Cardoso, R.A. *et al.* Effects of ethanol on recombinant human neuronal nicotinic acetylcholine receptors expressed in *Xenopus* oocytes. *J. Pharmacol. Exp. Ther.* **289**, 774–780 (1999).
4. Zhou, Q. & Lovinger, D.M. Pharmacologic characteristics of potentiation of 5-HT3 receptors by alcohols and diethyl ether in NCB-20 neuroblastoma cells. *J. Pharmacol. Exp. Ther.* **278**, 732–740 (1996).
5. Harris, R.A., Trudell, J.R. & Mihic, S.J. Ethanol's molecular targets. *Sci. Signal.* **1**, re7 (2008).
6. Wick, M.J. *et al.* Mutations of gamma-aminobutyric acid and glycine receptors change alcohol cutoff: evidence for an alcohol receptor? *Proc. Natl. Acad. Sci. USA* **95**, 6504–6509 (1998).
7. Lewohl, J.M. *et al.* G protein–coupled inwardly rectifying potassium channels are targets of alcohol action. *Nat. Neurosci.* **2**, 1084–1090 (1999).
8. Kobayashi, T. *et al.* Ethanol opens G protein–activated inwardly rectifying K^+ channels. *Nat. Neurosci.* **2**, 1091–1097 (1999).
9. Covarrubias, M., Vyas, T.B., Escobar, L. & Wei, A. Alcohols inhibit a cloned potassium channel at a discrete saturable site. Insights into the molecular basis of general anesthesia. *J. Biol. Chem.* **270**, 19408–19416 (1995).
10. Blednov, Y.A., Stoffel, M., Alva, H. & Harris, R.A. A pervasive mechanism for analgesia: activation of GIRK2 channels. *Proc. Natl. Acad. Sci. USA* **100**, 277–282 (2003).
11. Blednov, Y.A., Stoffel, M., Chang, S.R. & Harris, R.A. Potassium channels as targets for ethanol: studies of G protein–coupled inwardly rectifying potassium channel 2 (GIRK2) null mutant mice. *J. Pharmacol. Exp. Ther.* **298**, 521–530 (2001).
12. Reuveny, E. *et al.* Activation of the cloned muscarinic potassium channel by G protein βγ-subunits. *Nature* **370**, 143–146 (1994).
13. Wickman, K.D. *et al.* Recombinant G protein βγ-subunits activate the muscarinic-gated atrial potassium channel. *Nature* **368**, 255–257 (1994).
14. Huang, C.L., Slesinger, P.A., Casey, P.J., Jan, Y.N. & Jan, L.Y. Evidence that direct binding of G βγ to the GIRK1 G protein–gated inwardly rectifying K^+ channel is important for channel activation. *Neuron* **15**, 1133–1143 (1995).
15. Kunkel, M.T. & Peralta, E.G. Identification of domains conferring G protein regulation on inward rectifier potassium channels. *Cell* **83**, 443–449 (1995).
16. Krapivinsky, G. βγ binding to GIRK4 subunit is critical for G protein–gated K^+ channel activation. *J. Biol. Chem.* **273**, 16946–16952 (1998).
17. He, C., Zhang, H., Mirshahi, T. & Logothetis, D.E. Identification of a potassium channel site that interacts with G protein βγ subunits to mediate agonist-induced signaling. *J. Biol. Chem.* **274**, 12517–12524 (1999).
18. Ivanina, T. *et al.* Mapping the Gβγ-binding sites in GIRK1 and GIRK2 subunits of the G protein–activated K^+ channel. *J. Biol. Chem.* **278**, 29174–29183 (2003).
19. Finley, M., Arrabit, C., Fowler, C., Suen, K.F. & Slesinger, P.A. βL-βM loop in the C-terminal domain of G protein–activated inwardly rectifying K^+ channels is important for G(βγ) subunit activation. *J. Physiol. (Lond.)* **555**, 643–657 (2004).
20. Hara, K., Lewohl, J.M., Yamakura, T. & Harris, R.A. Mutational analysis of ethanol interactions with G protein–coupled inwardly rectifying potassium channels. *Alcohol* **24**, 5–8 (2001).
21. Pegan, S., Arrabit, C., Slesinger, P.A. & Choe, S. Andersen's syndrome mutation effects on the structure and assembly of the cytoplasmic domains of Kir2.1. *Biochemistry* **45**, 8599–8606 (2006).
22. Kruse, S.W., Zhao, R., Smith, D.P. & Jones, D.N. Structure of a specific alcohol-binding site defined by the odorant binding protein LUSH from *Drosophila melanogaster*. *Nat. Struct. Biol.* **10**, 694–700 (2003).
23. Nishida, M. & MacKinnon, R. Structural basis of inward rectification: cytoplasmic pore of the G protein–gated inward rectifier GIRK1 at 1.8 Å resolution. *Cell* **111**, 957–965 (2002).
24. Pegan, S. *et al.* Cytoplasmic domain structures of Kir2.1 and Kir3.1 show sites for modulating gating and rectification. *Nat. Neurosci.* **8**, 279–287 (2005).

25. Inanobe, A., Matsuura, T., Nakagawa, A. & Kurachi, Y. Structural diversity in the cytoplasmic region of G protein–gated inward rectifier K^+ channels. *Channels (Austin)* **1**, 39–45 (2007).
26. Rishal, I., Porozov, Y., Yakubovich, D., Varon, D. & Dascal, N. $G\beta\gamma$-dependent and $G\beta\gamma$ -independent basal activity of G protein–activated K^+ channels. *J. Biol. Chem.* **280**, 16685–16694 (2005).
27. Vivaudou, M. *et al.* Probing the G-protein regulation of GIRK1 and GIRK4, the two subunits of the KACh channel, using functional homomeric mutants. *J. Biol. Chem.* **272**, 31553–31560 (1997).
28. Zhang, H., He, C., Yan, X., Mirshahi, T. & Logothetis, D.E. Activation of inwardly rectifying K^+ channels by distinct PtdIns(4,5)P2 interactions. *Nat. Cell Biol.* **1**, 183–188 (1999).
29. Zhou, W., Arrabit, C., Choe, S. & Slesinger, P.A. Mechanism underlying bupivacaine inhibition of G protein–gated inwardly rectifying K^+ channels. *Proc. Natl. Acad. Sci. USA* **98**, 6482–6487 (2001).
30. Jenkins, A. *et al.* Evidence for a common binding cavity for three general anesthetics within the $GABA_A$ receptor. *J. Neurosci.* **21**, RC136 (2001).
31. Huang, C.L., Feng, S. & Hilgemann, D.W. Direct activation of inward rectifier potassium channels by PIP_2 and its stabilization by $G\beta\gamma$. *Nature* **391**, 803–806 (1998).
32. Peoples, R.W. & Ren, H. Inhibition of *N*-methyl-d-aspartate receptors by straight-chain diols: implications for the mechanism of the alcohol cutoff effect. *Mol. Pharmacol.* **61**, 169–176 (2002).
33. Dildy-Mayfield, J.E., Mihic, S.J., Liu, Y., Deitrich, R.A. & Harris, R.A. Actions of long chain alcohols on $GABA_A$ and glutamate receptors: relation to *in vivo* effects. *Br. J. Pharmacol.* **118**, 378–384 (1996).
34. Ramaswamy, S., Eklund, H. & Plapp, B.V. Structures of horse liver alcohol dehydrogenase complexed with NAD+ and substituted benzyl alcohols. *Biochemistry* **33**, 5230–5237 (1994).
35. Svensson, S., Hoog, J.O., Schneider, G. & Sandalova, T. Crystal structures of mouse class II alcohol dehydrogenase reveal determinants of substrate specificity and catalytic efficiency. *J. Mol. Biol.* **302**, 441–453 (2000).
36. Weinhold, E.G. & Benner, S.A. Engineering yeast alcohol dehydrogenase. Replacing Trp54 by Leu broadens substrate specificity. *Protein Eng.* **8**, 457–461 (1995).
37. Thode, A.B., Kruse, S.W., Nix, J.C. & Jones, D.N. The role of multiple hydrogen-bonding groups in specific alcohol binding sites in proteins: insights from structural studies of LUSH. *J. Mol. Biol.* **376**, 1360–1376 (2008).
38. Lu, T. *et al.* Probing ion permeation and gating in a K^+ channel with backbone mutations in the selectivity filter. *Nat. Neurosci.* **4**, 239–246 (2001).
39. Nishida, M., Cadene, M., Chait, B.T. & MacKinnon, R. Crystal structure of a Kir3.1-prokaryotic Kir channel chimera. *EMBO J.* **26**, 4005–4015 (2007).
40. Yi, B.A., Lin, Y.F., Jan, Y.N. & Jan, L.Y. Yeast screen for constitutively active mutant G protein–activated potassium channels. *Neuron* **29**, 657–667 (2001).
41. Sadja, R., Smadja, K., Alagem, N. & Reuveny, E. Coupling $G\beta\gamma$ -dependent activation to channel opening via pore elements in inwardly rectifying potassium channels. *Neuron* **29**, 669–680 (2001).
42. Jin, T. *et al.* The $\beta\gamma$ subunits of G proteins gate a K^+ channel by pivoted bending of a transmembrane segment. *Mol. Cell* **10**, 469–481 (2002).
43. Sarac, R. *et al.* Mutation of critical GIRK subunit residues disrupts N- and C-termini association and channel function. *J. Neurosci.* **25**, 1836–1846 (2005).
44. Riven, I., Kalmanzon, E., Segev, L. & Reuveny, E. Conformational rearrangements associated with the gating of the G protein–coupled potassium channel revealed by FRET microscopy. *Neuron* **38**, 225–235 (2003).
45. Ford, C.E. *et al.* Molecular basis for interactions of G protein $\beta\gamma$ subunits with effectors. *Science* **280**, 1271–1274 (1998).

ONLINE METHODS

Molecular biology and cell culture. cDNAs for mouse GIRK2c[46] (GIRK2c is referred to as GIRK2 in this study for clarity), rat GIRK4 (ref. 16), mouse IRK1 (ref. 24)[24], human m2R[46] and bovine m-Phos[26] were subcloned into pcDNA3.1 vector (Invitrogen). GIRK4* contains a S143T mutation in the pore-helix[27]. Point mutations were introduced by a Quickchange site-directed mutagenesis kit (Stratagene). GIRK2-PIP_2 mutant was created by the overlap-PCR method[47]. Briefly, a region of GIRK2-D228-L234 was replaced with the homologous region of IRK1-N216-L222; this region contains seven amino acids in the βC-βD region that have previously been implicated in PIP_2 binding[28,29] (we refer to this mutant as GIRK2-PIP_2). All mutations were confirmed by DNA sequencing. HEK-293T cells were cultured in DMEM supplemented with 10% fetal bovine serum (vol/vol) and 1× Glutamax (Invitrogen) in a humidified 37 °C incubator with 5% CO_2. Cells were plated in 12-well dish and transiently transfected with DNA using Lipofectamine 2000 (Invitrogen). Cells were replated to 12-mm glass coverslips coated with poly-D-lysine (20 μg ml^{-1}) 12–24 h after transfection.

Detection of channels expressed on membrane surface. GIRK2c and mutant channels were engineered with an extracellular HA epitope inserted between I126 and E127 for immunohistochemical detection with antibodies to HA[46]. HEK-293T cells were transfected with 0.5 μg of channel cDNA and examined 24–48 h after transfection. Cells were washed with 1× Dulbecco's phosphate buffer saline (DPBS, Invitrogen), fixed with 2% paraformaldehyde (wt/vol) in 1× DPBS for 10 min and rinsed with 1× DPBS (at 22–25 °C). To label surface channels, we incubated cells with blocking buffer (3% BSA in 1× DPBS) for 1 h and then with mouse antibody to HA (1:400 in blocking buffer, Covance) for 2 h at 22 °C. To label cytoplasmic channels, cells were rinsed with 1× DPBS, permeabilized with 0.25% Triton X-100 (Sigma) in blocking buffer for 10 min at 22 °C and incubated with blocking buffer for 1 h. Cells were then incubated with rabbit antibody to GIRK2 (1:200 in blocking buffer, Alomone) for 2 h. Following rinses in 1× DPBS, cells were incubated with fluorescent secondary antibodies, antibody to mouse Alexa-647 and antibody to rabbit Alexa-488 (1:300, Invitrogen), for 1 h in the dark. Cells were rinsed with 1× DPBS, mounted on microscope slides using Progold anti-fading reagent (Invitrogen) and both fluorophores were imaged with a Leica TSC SP2 AOBS laser confocal microscope.

Whole-cell patch-clamp electrophysiology. HEK-293T cells were transfected with 0.2 μg of channel cDNA and 0.04 μg of enhanced yellow fluorescent protein cDNA to identify transfected cells. For some experiments, 0.8 μg of m2R and 0.8 μg of m-Phos cDNA were also transfected. Whole-cell patch-clamp recordings were performed 24–72 h after transfection. Borosilicate glass electrodes (Warner Instruments) of 5–7 mΩ were filled with intracellular solution (130 mM KCl, 20 mM NaCl, 5 mM EGTA, 2.56 mM K_2ATP, 5.46 mM $MgCl_2$, 0.30 mM Li_2GTP and 10 mM HEPES, pH 7.4). Extracellular 20K solution contained 20 mM KCl, 140 mM NaCl, 0.5 mM $CaCl_2$, 2 mM $MgCl_2$ and 10 mM HEPES (pH 7.4). Alcohols (0.1–300 mM), carbachol (5 μM) or $BaCl_2$ (1 mM) were diluted into the 20K solution and applied directly to the cell with a rapid, valve-controlled perfusion system (Warner Instruments, VC6, MM-6 manifold). All of the chemicals that we used for our electrophysiology experiments were purchased from Sigma-Aldrich. Whole-cell patch-clamp currents were recorded using an Axopatch 200B (Molecular Devices, Axon Instruments) amplifier. Currents were adjusted electronically for cell capacitance and series resistance (80–100%), filtered at 1 kHz with an 8-pole Bessel filter and digitized at 5 kHz with a Digidata 1200 interface (Molecular Devices, Axon Instruments). Currents were elicited with voltage ramp protocol, from –100 mV to +50 mV, delivered at 0.5 Hz. Currents were measured at –100 mV and converted to current density (pA pF^{-1}) by dividing with the membrane capacitance. Basal K^+ currents (Ba^{2+} sensitive) were quantified at –100 mV by applying 1 mM $BaCl_2$ in 20K and measuring the amplitude of the Ba^{2+}-inhibited current. Alcohol- and carbachol-modulated currents were measured at −100 mV by averaging current from two consecutive sweeps on reaching steady state and subtracting the mean basal current before and after the application of the modulator. Pooled data are presented as mean ± s.e.m. and evaluated for statistical significance ($P < 0.05$) using a one-way ANOVA, followed by Bonferroni multiple comparison *post hoc* test. To determine the IC_{50}, we fitted the inhibition curves with the Hill equation ($y = \frac{1}{1+(\frac{x}{c})^b}$), where y is fraction of current remaining, x is the concentration of alcohol, b is the Hill coefficient and c is the IC_{50} (the concentration of alcohol that produces 50% inhibition).

Structural analysis. Molecular representations were made using PyMOL (DeLano Scientific) with PDB files 2GIX (IRK1-MPD), 2E4F (GIRK2) and 2QKS (Kirbac1.3-GIRK1). The cavity of the IRK1-MPD pocket was calculated using CASTp server[48] with a 1.4-Å probe radius. L245W was modeled in the IRK1-MPD structure by optimizing the best rotamer position for Trp using PyMOL software. Molecular volume estimates for amino acid side-chains were based on reported values[49].

46. Clancy, S.M. *et al.* Pertussis toxin–sensitive Galpha subunits selectively bind to C-terminal domain of neuronal GIRK channels: evidence for a heterotrimeric G protein–channel complex. *Mol. Cell. Neurosci.* **28**, 375–389 (2005).
47. Ho, S.N., Hunt, H.D., Horton, R.M., Pullen, J.K. & Pease, L.R. Site-directed mutagenesis by overlap extension using the polymerase chain reaction. *Gene* **77**, 51–59 (1989).
48. Dundas, J. *et al.* CASTp: computed atlas of surface topography of proteins with structural and topographical mapping of functionally annotated residues. *Nucleic Acids Res.* **34**, W116–118 (2006).
49. Harpaz, Y., Gerstein, M. & Chothia, C. Volume changes on protein folding. *Structure* **2**, 641–649 (1994).